Open Access
Stechnolock: Annals of Bioremediation and Biodegradation
RESEARCH ARTICLE

Plasma-Activated Water, A Green Technology for the Simultaneous Desorption and Removal of Organic Pollutants: Case of Methylene Blue Dye

Georges Kamgang-Youbi[1*], Moïse Fouodjouo[1], Elsie Acayanka[1], Serge A Djepang[2], Roger K K Ndounglha[1], Samuel Laminsi[1]

[1]Research Group of Physicochemistry of Environment, Department of Inorganic Chemistry, University of Yaoundé I, P.O. Box 812, Yaoundé, Cameroon.

[2]University Institute of Technology, University of Ngaoundéré, P.O. Box 455 Ngaoundéré, Cameroon

***Corresponding author:** Georges Kamgang-Youbi, Research Group of Physicochemistry of Environment, Department of Inorganic Chemistry, University of Yaoundé I, P.O. Box 812, Yaoundé, Cameroon, Tel: , E-mail: kamyougeo@yahoo.fr/drkamgangyoubigeorges@gmail.com

Citation: Georges Kamgang-Youbi, Moïse Fouodjouo, Elsie Acayanka, Serge A Djepang, Roger K K Ndounglha et al. (2022) Plasma-activated water, a green technology for the simultaneous desorption and removal of organic pollutants : case of methylene blue dye. Stech: Ann Biorem Biodegrad 1: 102

ABSTRACT

Methylene blue (MB) and Moabi sawdust (MS) were respectively employed as organic pollutant and adsorbent to evaluate the desorption capability of plasma activated water (PAW). MS effectively adsorbed MB dye in aqueous solution with efficiency of at least of 94% in the conditions tested with equilibrium time of 20 min. The adsorption was rapid at the beginning of the process and was driven by electrostatic interactions. Kinetic investigations showed that adsorption followed better a pseudo-second-order adsorption kinetic. A new method for dye desorption from MB-loaded-MS was tested using PAW, an ionic chemical solution obtained by exposing distilled water to humid air glidarc plasma. This eco-friendly solution was found to be effective with efficiency of 48% after 60 min of contact. MB desorption from MS was found to be spontaneous and endothermic process, with kinetic data also fitted pseudo-second-order model. pH study showed that PAW effect was primarily due to its acidic pH (3). Supplementary analysis showed that during desorption process, MB was concomitantly eliminated by PAW, thus allowing a regenerated adsorbent as efficient as the virgin one. Indeed, MB adsorption onto MS remained effective after three adsorption/desorption cycles: the adsorption efficiency slightly decreased from 96% to 93% while the desorption efficiency increased from 48% to 60%. Overall, this study has demonstrated that MS is a promising sorbent for the removal of MB dye, and that the ionic liquid PAW can be a green technology to regenerate efficiently wood sorbents.

Keywords:Adsorption; Desorption; Methylene blue; Plasma activated water; Wood sawdust

Introduction

The growing demand for basic human needs has led to an industrialization that is not always under control from the point of view of the waste produced, especially for developing countries. An example of discharges frequently encountered is the category of organic pollutants present in wastewater and more particularly dyes. Indeed, during manufacturing in industries such as textile, leather, paper, plastics, etc., about 15-50 % of reactive entrance dyes is lost during dyeing as effluents. Only by the effect of their color, dyes already highlight the presence of pollution: even very low concentrations of dyes in water (less than 1 ppm for some dyes) are highly visible and not recommended [1]. Due to complex molecular structure, textile wastewaters containing dyes are poorly biodegradable [2, 3]. Considering the use of large quantities of these non-biodegradable chemicals by humans, it is necessary to remove dyes from colored wastewaters before their discharge.

The literature presents a wide range of treatment technologies for dye removal including biological, physical, and chemical. Indeed, the main platforms of database of scientific research provide around 260 000 studies on dyes removal over the past decade, including approximately 23 000 for only 2021. The drawbacks and the advantages of each method were presented [4]. Adsorption, a physicochemical technique is the most widespread in terms of ease of its implementation, and design simplicity. Various kinds of adsorbents were employed for the removal of dye in solution, such as activated carbon [5], zeolites [6, 7], metal oxides [8], clays [9, 10], agriculture residues [1, 11], or waste sawdust [12]. The two later are considered as low-cost adsorbents in contrary of activated carbon for example, which production requires more complicated stages (carbonization, impregnation, chemical additives, etc.). Generally, with these low-cost adsorbents, adsorption process occurs through the affinity between polar functional groups of lignin and cellulose in biosorbent and dye molecules. The use of low-cost adsorbents, as eco-friendly technology for efficient dyes removal, has considerably increased in the last decade. Without being exhaustive, we can cite date palm leaves [13], paradise tree seeds [14], waste material of carrot [15], citrus limetta peel waste [16], breadnut peel [17], garlic straw [18], sawdust beech and red wood [19], timber sawdust [20], *Eucalyptus* sawdust [21], longan shell [22], white pine sawdust [23], *Mansonia* wood sawdust [24], carica papa wood [25], which have brought satisfactory results for the methylene blue (MB) dye removal from aqueous solutions. MB is a cationic dye which has been widely used including coloring paper, dyeing cottons, temporary hair colorant, wools and coating for paper stock. Eliminating MB from a waste is important because its acute exposure causes increased heart rate, vomiting, shock, cyanosis, and tissue necrosis in humans. As other basic dyes, MB can also cause allergic dermatitis, mutations, and skin diseases like cancer and psoriasis [26]. This dye is known for its strong adsorption onto solids [27], and it very often serves as a model pollutant for removing organic contaminants and colored bodies from aqueous solutions so far [27, 28].

In developing countries, wood sawdust is in most cases burned or used for cooking, and therefore contributes to the greenhouse effect due to the large amount of CO_2 released. If sawdust could be used as adsorbent, both the environment protection and wooden industry could benefit**.** Moabi (*Baillonella toxisperma*), also called African pear wood is a species of tree in the family *Sapotaceae*, commonly found in the Bassin of Congo forests. Moabi is a hard wood used for joinery and carpentry in exterior applications. Its uniform reddish-brown color and fine grain make it popular for veneer, furniture, decorative uses, and flooring. Report of Nko'o et al. [29] revealed that Moabi sawdust is essentially composed of cellulose (40.5%), lignin (29.6%), and hemicellulose (14.9%). Hence, the utilization of such waste could be interesting in pollutant adsorption. Therefore, as there is a constant search for cheaper substitutes, the performance and capability of Moabi sawdust for the adsorptive removal of MB from aqueous solution constituted the first aim of this study.

Although adsorption is a priori simple method to implement, it may prove to be insufficient under certain conditions. In fact, adsorption is not a destructive method of pollutant, given that its transfer pollutant from water to another phase. However, to achieve complete dye removal, relatively huge amounts of sawdust are required. The resulting polluted sawdust can present a sludge disposal problem. The pollutant-loaded-material constitutes a secondary pollution. It may therefore be necessary to regenerate or "purify" the adsorbent by desorbing the pollutant. The regenerated adsorbent can then be employed for other subsequent re-uses. Literature demonstrated that mineral and organic chemicals such as hydrochloric acid HCl [14, 25], acetic acid CH_3COOH [16], sodium chloride NaCl [10, 20], or calcium chloride $CaCl_2$ [10] can be used for MB desorption. All these desorption methods are not eco-friendly, and their efficiencies of regeneration depends on the types of organics to be removed. A new route for pollutant desorption can be achieved by plasma activated water (PAW).

PAW is obtained by exposing a distilled solution (initially devoid of any action) to plasma for a period. Plasma, the fourth fundamental state of matter, can be defined as an ionized gas, which includes various reactive species depending on the gas. Based on the difference of temperature between electrons and ions, there are two types of plasma: thermal plasmas and non-thermal plasmas. Non-thermal plasma is a partially ionized gas with electron temperatures much higher than ion temperatures. The high-energy electrons and low-energy molecular species can initiate reactions in the plasma volume without excessive heat in contrary of thermal plasmas. Concerning the treatment of organic pollutants, the technology plasma belongs to the « Advanced oxidation processes (AOP) », which refer to a set of techniques aimed at *in situ* generation of very powerful oxidants such as hydroxyl radicals $HO^{\bullet}$, atomic oxygen O, hydrogen peroxide H_2O_2, hydroperoxyl radicals $^{\bullet}O_2H$. Gliding electrical discharge (Glidarc) is an easy and suitable technique of generation of non-thermal plasma [30]. Initially developed for the treatment of gases, this technology is also very well suited to the treatment of liquids as detailed in the review paper of Brisset et al. [30]. When the gas is humid air, the chemistry of the glidarc plasma involves the production of $NO^{\bullet}$ and $HO^{\bullet}$ radicals as main reactive species [31]. $NO^{\bullet}$ radical is known to be involved in acid effects and $HO^{\bullet}$ radical is involved in the oxidation effects due to its high redox potential ($E^{\circ}_{HO/H2O}$ = 2.85V/SH). Moreover, these primary species are precursors of other entities such as the reactive oxygen species (ROS) H_2O_2, $^{\bullet}O_2H$; the reactive nitrogen species (RNS) NO_2, HNO_2, NO_2^-, NO_3^-, ONOOH, $ONOO^-$, and the ions O_2^+, O^+, N_2^+, N^+ [30, 32]. These species are for the most part soluble in aqueous solution and exhibit acid–base and oxidation–reduction properties, which explain the reactivity of the subsequent PAW. So, glidarc humid air plasma can transform initial distilled water to a powerful chemical solution containing ROS and RNS. We first evidenced the PAW concept for bacterial inactivation purpose [33] and generalized it for microorganism destruction [34-36]. Recently, we showed that this ionic solution can be used in the decontamination of surface (e.g., stainless steel and polyethylene) without affecting their topographic properties [37]. As an efficient desorbing agent should desorb the dye without destruction of the biomass structure and functional groups, PAW can be a promising candidate. To the best of our knowledge, there is no report focused on the use of PAW in pollutant desorption process. Moreover, using PAW can be considered as green technology as no chemical was adding. The second part of this current study is an attempt to utilize this "newly concept" as a desorbing agent of MB from wood sawdust. The regeneration of sorbents is critical to keep the treatment cost low, minimizing the disposal problem by discarding the adsorbents safely. Adsorption-desorption cycles were carried out to verify the reusability of the adsorbents.

Materials and Methods

Adsorbate and reagents

MB ($C_{16}H_{18}N_3SCl$) laboratory grade was supplied in powder form by Merck and was used without further purification for the preparation of synthetic solution. The stock solution of 1000 mg/L was prepared by dissolving accurately weighed amounts of MB in 1000 mL distilled water. The experimental solution was prepared by diluting the stock solution with distilled water when necessary. Analytical reagents grade each HCl, NaOH, NaCl, HNO_3, and CH_3OH were also used in the present investigation.

The adsorbent

MS collection and preparation

MS was collected from a local sawmill in Yaoundé, Cameroon, and was sun-dried for a week. After drying, MS was crushed as finely as possible, and then sieved in the size ≤ 120 µm. After collection and sieving, 10 g of the reddish-brown colored sawdust was soaked into a solution of methanol (water/methanol: 7/3) for 2 hours to remove the extractables and impurities. After washing thoroughly with distilled water until neutral pH, the sawdust was sun-dried again for a day, and then in an electric oven at 105 °C for 2 hours. The obtained biosorbent MS was stored in an airtight plastic container to avoid moisture.

Characterization of adsorbent

The functional groups on the surface of MS were identified by Fourier Transform Infrared (FTIR) spectroscopy in the wave range of 4000-400 cm^{-1} using using a Perkin Elmer FT-IR (KBr pellets method) to determine surface functional groups.

The micro-morphology of MS material was obtained using high-resolution scanning electron microscopy (JEOL JSM-6701F, SEM-FEG).

The zero-point charge (pH at which the biosorbent surface has net electrically neutral) of MS was determined through the method proposed by Ofomaja and Ho [38] for wood sawdust. For this purpose, 50 mL of sodium chloride (0.1 M) was transferred to a series of 100 mL conical flasks and the initial pH of solutions was adjusted to the values of 2.0, 4.0, 6.0, 7.0, 8.0, 10.0 and 12.0 using either 0.1M HCl or 0.1M NaOH solution. Followed with that, 0.1 g of MS was added to each flask and shaken for 48 h with agitation speed of 120 rpm at the room temperature (298 K). Then the final solution pH (pH_f) was measured. The difference between the values of initial solution pH (pH_i) and final solution pH, noted ΔpH was plotted against pH_i. The zero-point charge (pH_{pzc}) was found from the intersection point of the resulting curve at which ΔpH is equal to zero.

Batch adsorption experiments

The adsorption experiments were carried out by batch process, in 250 mL Erlenmeyer flasks on thermostatic shaker. 0.1 g of MS was placed in the flask with 50 mL of MB solution of 20 $mg.L^{-1}$ initial concentration. The mixture was agitated at 150 rpm for an appropriate contact time at 298 K. After decantation and filtration, the residual MB concentration in the filtrate solution was determined by a direct spectrophotometric method. The absorbance of a sample was measured in a UV/Visible spectrophotometer (JENWAY 6705 UV/Vis) at a wavelength of 664 nm. Then, the concentration of MB in a sample was estimated using a calibration curve, concentration of the MB *vs*. absorbance. The calibration curve presented a linear behavior when the concentration of the MB ranged from 0 to 20 $mg.L^{-1}$. For the calculation of MB rate adsorption (*% Ads*) or removal percentage, and the quantity adsorbed at equilibrium per unit mass of biosorbent ($q_{e,ads}$ in mg/g), the following expressions were used:

$$\% Ads = \frac{C_0 - C_e}{C_0} \times 100 \quad (1)$$

$$q_{e,ads} = \frac{C_0 - C_e}{m} \times V \quad (2)$$

where V is the volume (L) of solution; C_0 is the initial MB concentration (mg/L) in contact with the adsorbent; C_e is the residual concentration (mg/L) after adsorption process and m is the mass (g) of MS.

The effect of pH was studied at pH range of 3.0−10.0 using 0.1 M NaOH or 0.1 M HCl to adjust the initial pH value. The effect of adsorbent dosage was studied by varying the mass of MS from 0.1 to 1.0 g.

Desorption experiments

Preparation of PAW solution

The technique employed to produce the desorbing solution was non-thermal plasma of glidarc batch reactor type, operating at atmospheric pressure. Humid air (flow rate: 650 $L.h^{-1}$) was used as the plasma gas. Fig. 1 illustrates the scheme of the experimental device.

The procedure for gas discharge has been described previously [39]. The glass treatment reactor was fitted with a circulating water jacket to prevent any thermal effect. Plasma activated water (PAW) was obtained by exposing 400 mL of distilled water to glidarc plasma for 5, 15, and 30 min and then used immediately as desorbing solution. The different solutions resulted were noted PAW-5, PAW-15, and PAW-30 for 5, 15, and 30 min of treatment respectively.

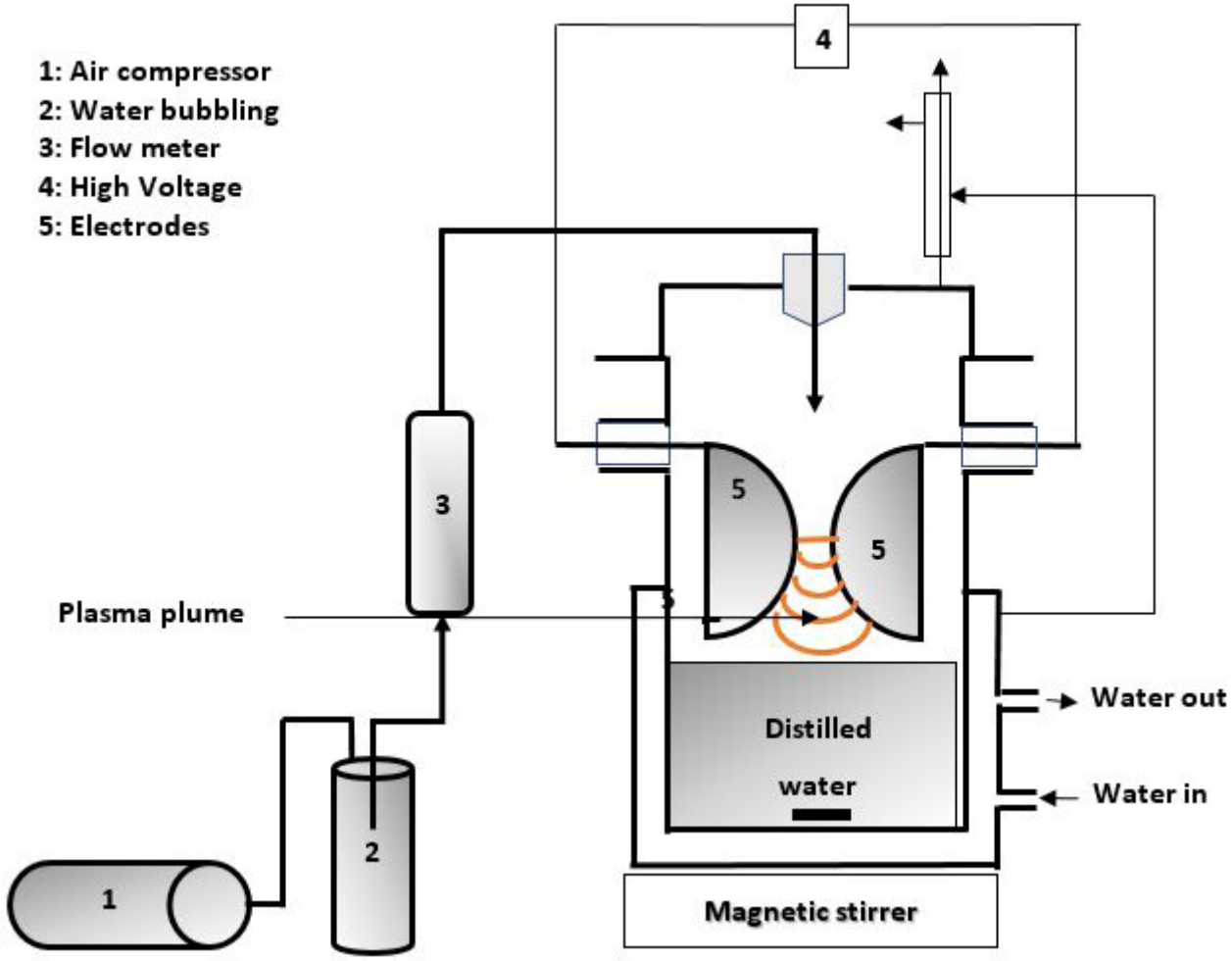

Figure: 1 Scheme of glidarc device for plasma activated water production

Procedure of desorption

The MB-loaded-MS after the adsorption process in the optimal conditions was separated and dried in an electric oven at 105 °C. Desorption studies were carried out at desired temperature (298, 313, 323, and 333 K) on thermostatic shaker as follows: 0.1 g of dried MB-loaded-MS were placed in 50 ml of PAW, and they were agitated at 150 rpm for an appropriate contact time at the desired temperature. Under these conditions, the MB is desorbed from MS to the solution and equilibrium was again attained. The MB rate desorption (*% Des*) and the MB dye desorption capacity ($q_{e,des}$) were calculated using Eqs. (3) and (4).

$$\% \, Des = \frac{C_f \times V}{m \times q_{e,ads}} \times 100 \qquad (3)$$

$$q_{e,des} = \frac{C_f \times V}{m} \qquad (4)$$

where, C_f is the MB dye concentration in the desorbing solution (mg.L^{-1}), V is the PAW volume (L), m is the dye-saturated-MS mass (g), $q_{e,ads}$ is the MB dye adsorption capacity (mg/g) and $q_{e,des}$ is the amount of dye desorbed per gram of dye saturated adsorbent at equilibrium (mg/g).

Reusability tests

To check the reusability of the MS, regeneration experiments were performed. After the desorption process, the MS was washed thoroughly with distilled water for several times until neutral pH, and then oven dried. The regenerated MS was analyzed for the reuse by subjecting for the further adsorption process as described in section 2.3. The adsorption followed with the desorption

process were performed up to three cycles, to examine the MB removal efficiency by MS under the regenerated conditions. The adsorption and desorption efficiencies were calculated by using Eq. (1) and Eq. (3) respectively.

Results and Discussion

MS characteristics

Fig. 2 (a) depicts the SEM image of MS with three magnifications (×1.000, ×1.500, ×5.00). The MS surface is heterogeneous, rough, and porous with the presence of intercellular voids in the form of circular cavities partially spaced. It is a suitable material for absorption of several substances.

FTIR spectrum (Fig. 2 (b)) shows the presence of main bands due to the functional groups common to lignocellulosic materials. A broad and intense band is observed around 3410 cm^{-1}, which corresponds to the elongation vibrations of the O-H bond. Around 2923 and 2800 cm^{-1}, there is double peak which correspond to the asymmetric elongation vibration of the CH and CH_2 (symmetric stretch) of the cellulose. The peak of C=O valence vibration of aldehydes, esters and carboxylic acids present in lignin and hemicellulose appears around 1731 cm^{-1}. The vibration at 1457 cm^{-1} can be attributed to the deformation (C=C) of the aromatic cycles of the lignin and at around 1060 cm^{-1}, there is a strong C-O band also confirms the lignin structure. Some other peaks appearing below 900 cm^{-1} are characteristics of the C-H group in the cellulose. All the observations are consistent with previous studies carried out on wood sawdust [14, 19, 23, 29].

A plot for the determination of pH_{pzc} was showed in Fig. 2 (c). The pH_{pzc} value of MS was found to be around 7.2. This indicates that the adsorbent surface has positive charge at pH < 7.2, net zero charge at pH = 7.2 and negative charge at pH > 7.2. This value is close to that of *Ayous* sawdust (pH_{pzc} = 6.5), another Cameroonian wood [40] and to that of *Mansonia* sawdust (6.91) determined by a similar method [38].

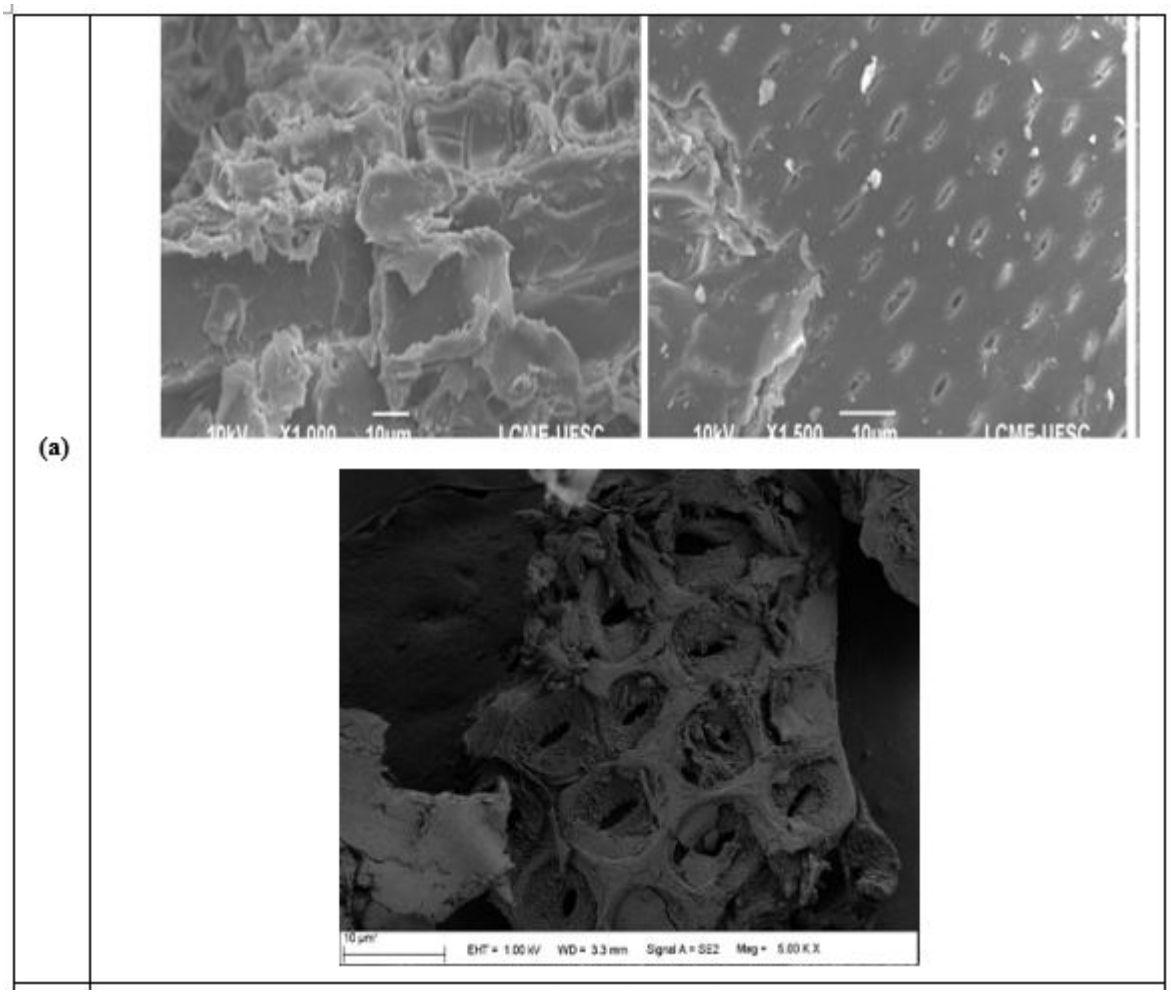

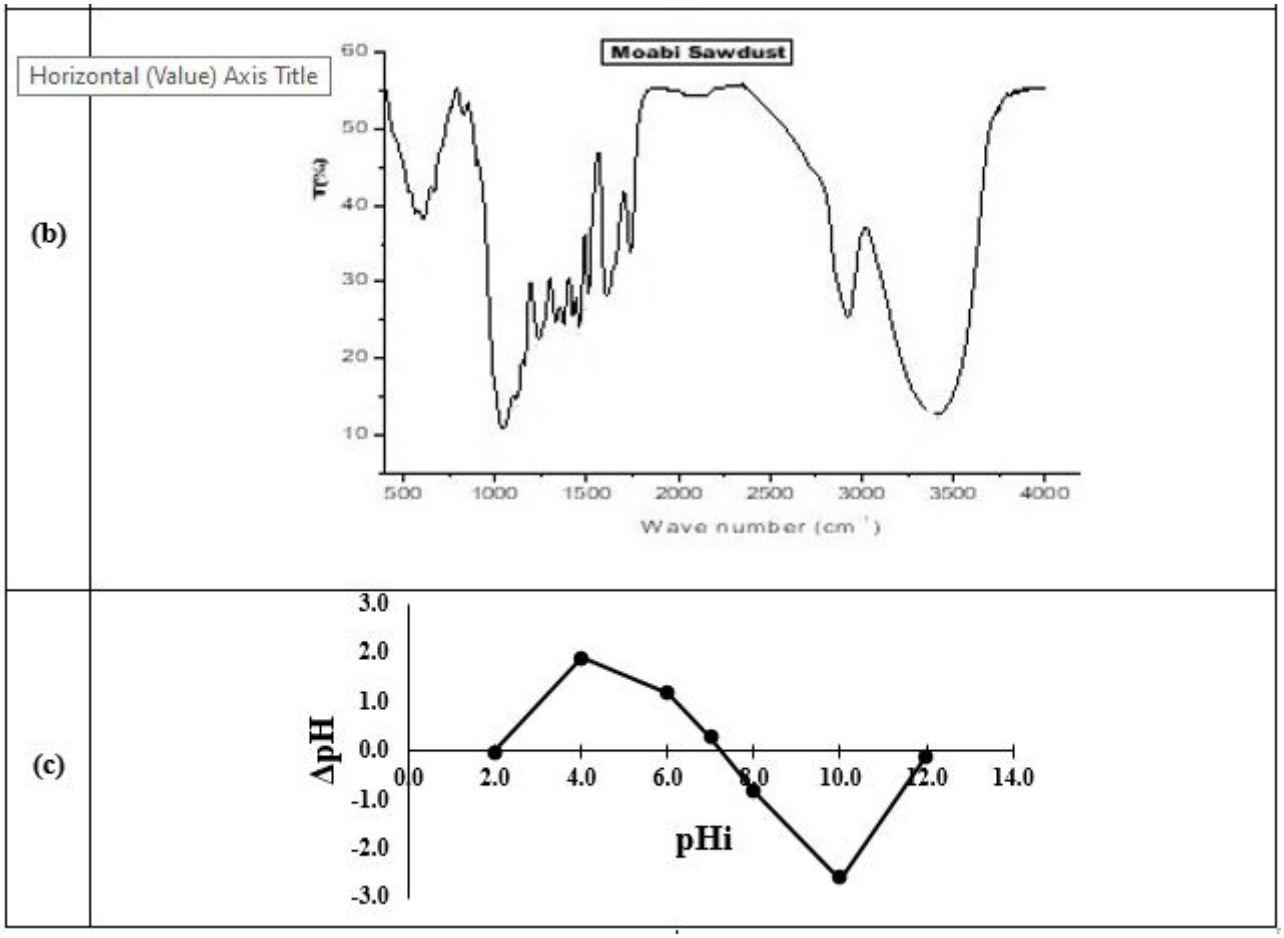

Figure :2 The characteristics of Moabi sawdust (a) SEM images with progressively increased magnification, (b) FT-IR spectra and (c) PZC determination.

Adsorption studies

Effect of adsorbent dose and contact time

The influence of the initial amount of adsorbent and contact time was studied at the pH of the solution without adjustment. Different amounts of MS were added into 50 mL of MB dye of 20 $mg.L^{-1}$ concentration and then mixture was stirred. After different predetermined contact times, the absorbance was measured. The variation in percentage removal of MB dye (*% Ads*) with contact time is shown in Fig. 3 for each MS dose.

First, the adsorption rate of MS increased rapidly during the first five minutes whatever the dose of the adsorbent, which indicated that MS adsorbs MB well. This fast adsorption indicates the presence of abundant readily accessible adsorption sites which were occupied by the first molecules of MB. A rapid uptake of adsorbate by an adsorbent is especially important when applied to wastewater treatment by means of adsorption, which signifies the efficacy of an adsorbent to be used in wastewater treatment. Then, between 5 and 45 min, the uptake rate remained almost constant, since the MS fixation sites were almost all occupied. The equilibrium state, characterized by approximate constant adsorbed MB amounts was independent of the mass of adsorbent and was approximately attained at 20 min.

The effect of adsorbent dose indicated a slight overall increase in the rate of adsorption when the dose increased from 0.1 to 0.3 g, due to an increase in the number of adsorption sites. Then, a slight decrease in the adsorption rate beyond this adsorbent dose was recorded. Indeed, for 20 min of contact, 95.98% for m = 0.1 g; 97.86% for m = 0.3 g; 97.40% for m = 0.5 g and 94.07% for m = 1.0 g were recorded. The slightly decreasing of adsorption rate beyond a mass of 0.3 g indicates probably the presence of another type of interaction between dye and sawdust. This behavior could be due to a competition between the fibers retaining dye fractions and the free fibers of the adsorbent which attract the latter, causing it to return to the solution reference [19]. Furthermore, as for

all the conditions tested, the rate is at least equal to 94%, it is not necessary to use mass higher than 0.1 g. In addition, the greatest adsorption capacity was obtained with 0.1 g ($q_{e,ads}$ = 9.60 mg/g). Therefore, 0.1g of MS, corresponding to a dose of 2 g.L^{-1}, was chosen for the successive experiments.

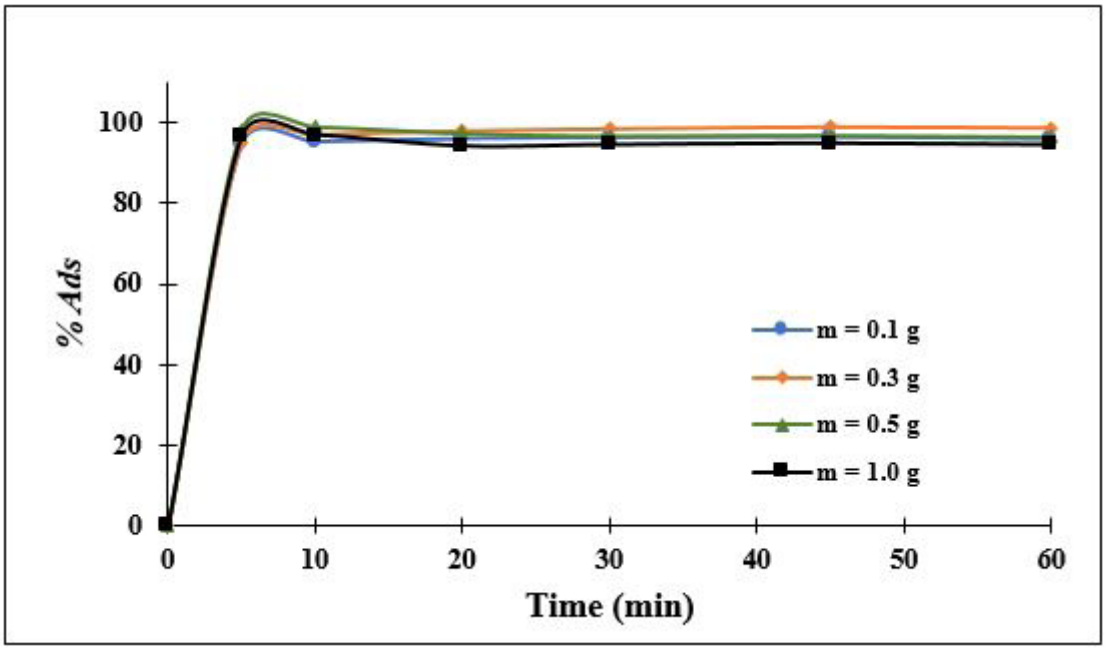

Figure :3 Effect of contact time on MB dye adsorption onto MS at different adsorbent dosages

Effect of initial pH

The effect of initial pH was studied by adjusting the initial pH of MB 20 mg.L^{-1} in the range 3.0-10.0. Prior to adsorption analysis, each dye solution with different pH condition was spectrophotometrically analyzed to ensure that λ_{max} remain unaltered. This observation implies that change in solution pH doesn't change the chemical structure of dye molecules, therefore the adsorption results solely due to adsorption process.

At ambient pH (7.5), 95.98% of MB was adsorbed for 20 min of contact (Fig. 4). As the pH decreases, there was a decrease in the amount of MB adsorbed and as the pH increases, there was an increase of adsorption percentage (Fig. 4). The effect was more pronounced in the pH range of 3–4.5 (from 91.81% for pH 4.5 to 83.19% for pH 3). This result is in accordance with different previous studies on MB adsorption onto low-cost adsorbents [17, 19, 20, 25] and the explanations of this behavior are generally related to the point of zero charge. We showed that the pH_{pzc} of MS was approximately 7.2, practically the neutral pH. At pH < pH_{pzc}, the protonation of carboxylate groups and the interactions between hydroxyl functions and protons occurred, so the surface of sawdust is positively charged. Consequently, electrostatic repulsions can prevent the efficient interaction between the protonated MS and the cationic dye MB. This effect can explain the low removal value for pH 3. Moreover, the pKa of MB is 3.8, so at pH =3, the undissociated MB$^{\circ}$ species predominates (86%) [23]. Therefore, the MB was predominantly adsorbed as MB$^{\circ}$ on MS at pH = 3. At pH > pH_{pzc}, the surface of MS become negatively charged and favors the uptake of cationic dye. According to Fig. 4, there was no significant difference on the amount of MB being adsorbed from ambient pH to pH 10. Hence, the ambient pH was chosen for all the other experiments in this study.

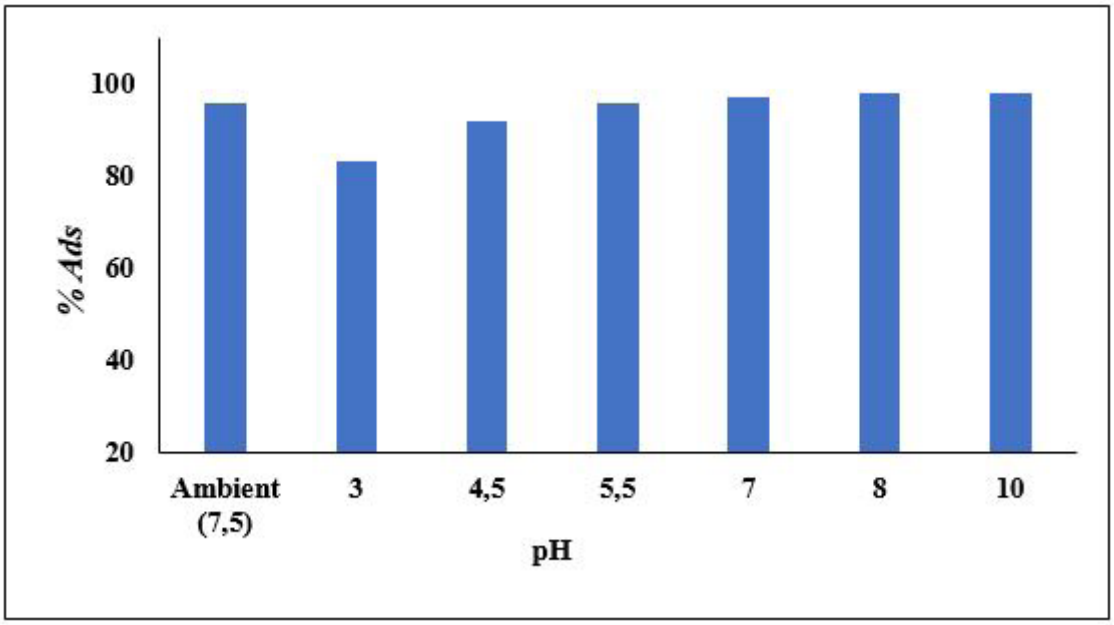

Figure :4 Effect of medium pH on the percentage removal of MB dye from aqueous solution using MS

Thermodynamic considerations

To determine whether the adsorption process occurs spontaneously, the energy and entropy factors were considered. The change in Gibbs free energy (ΔG°) is given by the Eq. (5):

$$\Delta G^{\circ} = -RT \ln (K_c) \qquad (5)$$

where ΔG° is the Gibbs free energy (J.mol^{-1}), R the universal gas constant (8.314 J.mol^{-1}.K^{-1}), T is the absolute temperature (K) and K_c is the equilibrium constant (C_{ads}/C_e). C_{ads} is the concentration of MB on adsorbent (mg.L^{-1}) and C_e is the equilibrium concentration of MB (mg.L^{-1}). Then, the enthalpy (ΔH°) and the entropy (ΔS°) can be calculated from the Van't Hoff Eq. (6):

$$\ln(K_c) = \frac{-\Delta H^{\circ}}{RT} + \frac{\Delta S^{\circ}}{R} \qquad (6)$$

The plot of ln (K_c) *vs.* (1/T), gave a straight line with a value of R^2 (0.9562) reasonably close to one (Fig. 5).

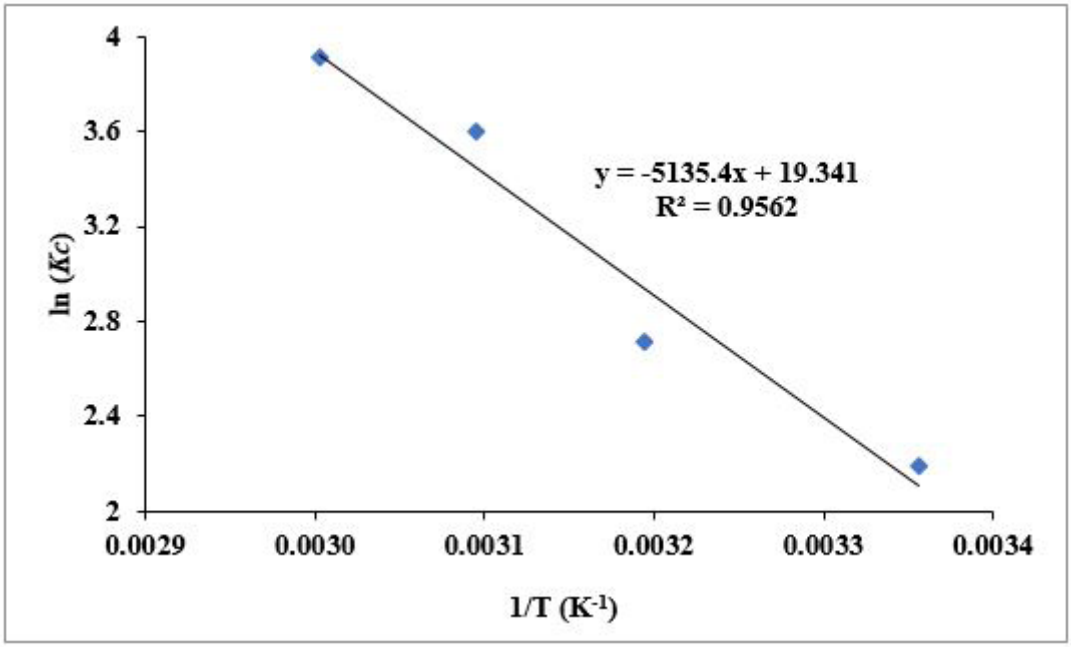

Figure :5 Plot of ln (Kc) vs 1/T for the determination of thermodynamic parameters of adsorption of MB dye onto MS

The calculation and intercept from the plot were used to estimate ΔH° and ΔS°, respectively (see Table 1).

The Gibbs free energy was found to be −5.22 kJ.mol^{-1} at 298 K, which indicates a favorable adsorption process that was spontaneous at ambient conditions (pH and temperature). The process was also spontaneous for the other temperatures tested. The value of ΔH° indicates an endothermic process, and the positive entropy change within the temperature range suggests that there would be an affinity of the MS towards MB, demonstrated by the increase in randomness at the adsorbate-solution interface during adsorption process. The increase in entropy is presumably due to gain of translational entropy by the dye molecules during adsorption process [16].

Temperature (K)	ΔH° (kJ.mol^{-1})	ΔS° (J.mol^{-1}.K^{-1})	ΔG° (kJ.mol^{-1})
298	42.69	160.79	− 5.22
313			− 7.64
323			− 9.24
333			− 10.85

Table :1 Thermodynamic parameters calculated for the adsorption of MB dye onto MS

Kinetics of adsorption

The kinetics of adsorption was carried out at the same temperatures used in the thermodynamic study above and in the following conditions: ambient pH, 0.1 g of MS and initial MB concentration 20 mg.L^{-1}, with contact time ranged from 0 to 45 min. The most famous ones for analysis of experimental data for adsorption kinetics are the pseudo-first-order, pseudo-second-order and Elovich models.

The pseudo-first-order model

Also called The Lagergren's kinetic model, this model has its significance in the adsorption rate constant determination based on the adsorption capacity. The pseudo-first-order kinetic model considered the assumption that the rate of change of the adsorbate removal with time leads to change in the adsorption capacity of the adsorbent. The mathematical expression of pseudo-first-order model was:

$$q_t = q_{e,ads}(1 - e^{-k_1 t}) \qquad (7)$$

This expression can be rearranged in the linearized form:

$$\ln(q_{e,ads} - q_t) = -k_1 t + \ln(q_{e,ads}) \qquad (8)$$

where, $q_{e,ads}$ (mg/g) and q_t (mg/g) are the amount of MB adsorbed at equilibrium and at time t (min), respectively and k_1 (min^{-1}) is the pseudo-first-order rate constant.

For the determination of the pseudo-first-order kinetic constants, plots of ln ($q_{e,ads}$ - q_t) *vs.* t were made and the constant values $q_{e,ads}$, k_1 were determined from the intercept and slope of the plot (not shown). The values of the coefficient of determination were found lower ($R^2 < 0.7$) for all the temperatures studied, and the theoretical adsorbed masses ($q_{e,\ adsI}$), were significantly different from the experimental ones. Therefore, the pseudo-first-order kinetic model failed to explain the adsorption of MB onto MS.

a) The pseudo-second-order model:

This model was proposed by Ho and McKay [41] and was expressed as:

$$q_t = \frac{t \cdot q_{e,ads}^2 \cdot k_2}{1 + k_2 \cdot q_{e,ads} \cdot t} \quad (9)$$

Eq. (9) could be linearized as:

$$\frac{t}{q_t} = \frac{t}{q_{e,ads}} + \frac{1}{k_2 \cdot q_{e,ads}^2} \quad (10)$$

k_2 (g/(mg·min)) is the pseudo-second-order rate constant; $q_{e,ads}$, q_t and t were previously defined. The adsorption data were plotted as t/q_t *vs.* t and giving linear plot as shown in Fig. 6.

From Table 2, it can be seen that the calculated adsorbed masses at equilibrium ($q_{e,adsII}$) are in good agreement with the experimental ones (q_e, *exp*): the maximum difference did not exceed 1.5%. Thus, these results suggest that the pseudo-second-order model best described the adsorption kinetics. Table 2 shows that the rate constant $q_{e,AdsII}$ increased with the temperature increase, thus confirms the endothermic process. Some previous studies based on the adsorption of MB to low-cost adsorbents also fitted the pseudo-second-order model [13, 15, 16, 20, 25]. The pseudo-second-order model assumes that the rate-limiting step might be chemical adsorption involving valence forces through sharing or exchange of electrons between adsorbent functional groups and adsorbate.

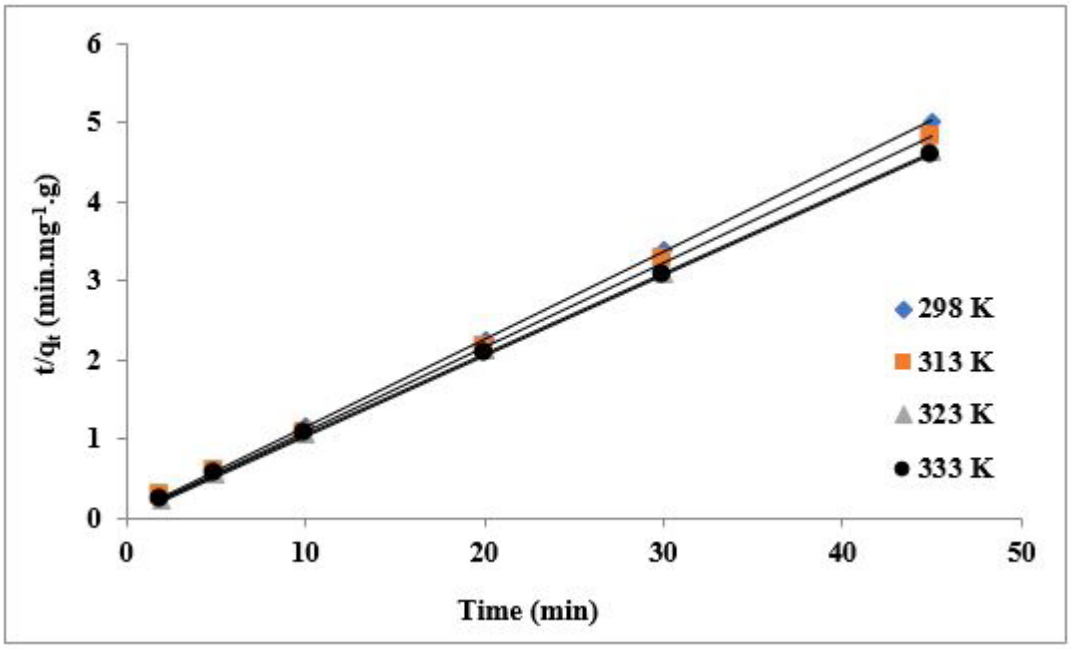

Figure :6 Plots of pseudo-second-order kinetic model for the adsorption of MB dye onto MS at different initial temperatures

T (K)	$q_{e,\,exp}$ (mg.g^{-1})	Pseudo-second-order			Elovich		
		k_2 (g/(mg.min))	R^2	$q_{e,\,adsII}$ (mg.g^{-1})	α (mg/(g.min))	β (g.mg^{-1})	R^2
298	9.01	0.25	0.9998	9.09	2.42	3.40×10^{7}	0.8986
313	9.38	0.37	0.9998	9.43	2.25	2.19×10^{7}	0.8297
323	9.73	0.28	0.9999	9.80	3.43	2.33×10^{12}	0.9747
333	9.81	0.36	0.9999	9.90	4.73	7.61×10^{17}	0.9763

Table :2 Pseudo-second-order and Elovich parameters at various initial temperatures for adsorption of MB dye onto MS

b) Elovich model

The Elovich model is based in assumption that the adsorption performance of chemisorption and heterogeneous systems [42]. The linearized form of the Elovich kinetic model represented as follows:

$$q_t = \frac{1}{\beta}\ln(t) + \frac{\ln(\alpha.\beta)}{\beta} \qquad (11)$$

where α indicates the initial rate of adsorption ($mg.g^{-1}.min^{-1}$) and β represents the Elovich constant, refers to the extent of surface coverage ($g.mg^{-1}$). The plot of q_t *vs.* ln *(t)* (not shown) gave the constant values of the Elovich kinetic model (Table 2). Globally, the value of α was higher at the higher temperature and the value of β increased with the increase of the temperature. However, the coefficient of determination value of Elovich kinetic model for the adsorption of MB using MS was found lower than that of the pseudo-second-order kinetic.

Desorption studies

The PAW solution

The PAW solution employed here is a chemical solution resulting of exposure of distilled water to glidarc humid air plasma. It is recalled that in the plume of the glidarc humid air plasma, the major species are the radicals $HO^{\cdot}$ and $NO^{\cdot}$. In solution, the $NO^{\cdot}$ radical oxidizes gradually to NO_2^- and then finally to NO_3^-, isomer of the transient species peroxynitrite $ONOO^-$. $HO^{\cdot}$ is rapidly dimerized to H_2O_2. These species are responsible for the acidification and oxidizing character of prepared PAW. Eqs. (13)–(19) were established to support the production of these chemical:

$$H_2O + e^- \rightarrow HO^{\cdot} + H^{\cdot} + e^- \qquad (13)$$

$$N_2 + e^- \rightarrow 2\,N + e^- \qquad (14)$$

$$N + O_2 \rightarrow NO^{\cdot} + O \qquad (15)$$

$$HO^{\cdot} + HO^{\cdot} \rightarrow H_2O_2 \qquad (16)$$

$$4\,NO^{\cdot} + O_2 + 2\,H_2O \rightarrow 4\,NO_2^- + 4\,H^+ \qquad (17)$$

$$NO_2^- + H_2O_2 \rightarrow ONOO^- + H_2O \qquad (18)$$

$$NO_2^- + 2\,HO^{\cdot} \rightarrow NO_3^- + H_2O \qquad (19)$$

In Table 3, we summarized some characteristics of PAW obtained at different exposure times. Compared to the initial distilled water, there were significantly change in the physicochemical parameters measured (pH, conductivity, salinity, dissolved oxygen). The pH, very important parameter in desorption of anionic or cationic dye was around 3 regardless the exposure time. The contents of PAW make it to be an ionic solution and thus can be used as desorbing agent like common HCl, NaOH, NaCl, etc….

Desorption with PAW

Desorption studies were carried out by introducing 0.1 g of MS-loaded-MB into 50 mL of PAW solution. The MB load was obtained in optimal condition i.e. 9.60 $mg.g^{-1}$. During shaking, the MB was gradually desorbed, and its concentration was measured. Fig. 7 showed the percentage of desorbed MB and the amount of MB desorbed per gram of MS for various contact times with PAW-30.

A control experiment, carried out using distilled water as desorbing agent, showed that less than 4% MB pre-adsorbed onto MS was desorbed (Fig. 7), showing most MB to be strongly bond to the MS. With PAW, a rapid desorption occurred in the first five min, then slowly between 10 and 20 min, and equilibrium stage from 20 to 60 min. Compared to the non-activated water, significantly higher 48.49% of adsorbed MB were released within 1 h.

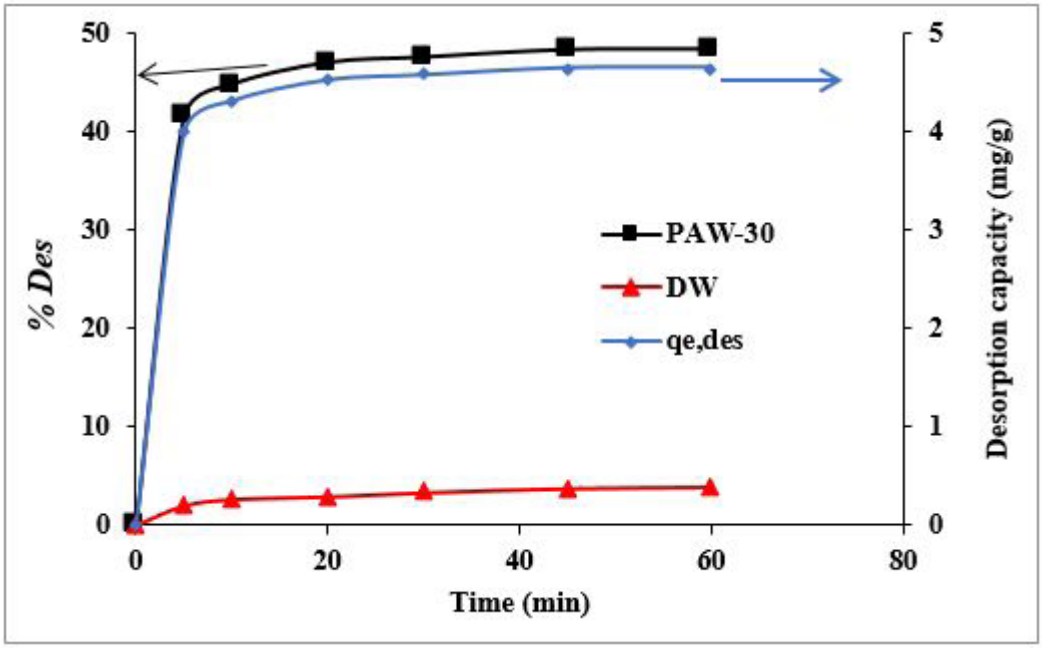

Figure :7 Desorption efficiency (%) and desorption capacity (mg/g) of MB dye from MS using PAW. Experiments with distilled water (DW) were added

The first observation that emerges to explain the desorbing ability of PAW is its acidic pH (Table 3). Indeed, Jeyagowri and Yamuna [14] used HCl 0.1 M for desorption of 32.1% MB from seed shell powder; Shakoor and Nasar [16] obtained similar results for desorption of MB from biosorbent citrus limetta. So, MB dye showed the acidic condition favors desorption. Recently, a study aimed to compare seventeen different chemical agents for MB desorption from brown macroalga, also showed that the acidic eluents were more efficient that neutral and alkaline [43]. That study revealed a desorption rate of 40.7% for HCl 1 M and 0% for NaOH 1 M. We showed in paragraph 3.2.2 that MB adsorption onto MS was most favorable in neutral and alkaline media and less favorable in acidic media; as desorption is a reverse process of adsorption, it seems evident that desorption was favorable in acidic conditions. Zheng et al. [44] also demonstrated the crucial role of pH during the recovery of methylene blue after adsorption from aqueous solution through ultrafiltration technique.

	Distilled water	PAW-5	PAW-15	PAW-30
Temperature (K)	295	298	300	301
pH	6.4	3.3	3.2	2.9
Dissolved oxygen (mg/L)	8.40	33.7	34.4	34.8
Electric conductivity (mS/cm)	< 0.05	0.343	0.746	0.883
Salinity (%)	0	0.02	0.04	0.05
Oxidation-reduction Potential (mV)	165	557	583	587

Table :3 Characteristics of PAW compared with those of the original distilled water

To effectively check the role of pH in PAW desorption of MB from MS, desorption experiment was carried out by replacing PAW solution with acidic solution (HCl) having the same pH as PAW. After 1 h of process, 4.60 mg/g of MB were desorbed, corresponding to 47.87% of pre-adsorbed MB (Fig. 8). As the plasma generates nitrogen oxides in activated water, one of the ultimate species of which is the NO_3^- ion [37], a comparison analysis was also carried out using nitrate solution at pH 3 (in fact, nitric acid) and the results indicated *%Des* of 41.68% for one hour of contact (Fig. 8). HCl and HNO_3 acting only by their protons released in solution, it is therefore clear that pH plays a fundamental role in desorption by PAW. At acidic pH, as there is an abundance of H^+ ions in solution, the desorption would result from a cation exchange between the H^+ protons and the MB^+ cations adsorbed on MS. Another reason might be the fact that under acidic conditions, the number of positively charged sites on the MS increases ($pH < pH_{pzc}$), thus desorption can easily occur by electrostatic repulsion between positively charged sites on MS and cationic dye molecules. Zhou et al. [45] also showed change in the pH value (from 6 to 2.7) of the regeneration system by cold atmospheric plasma of agricultural biomass used for adsorption of MB.

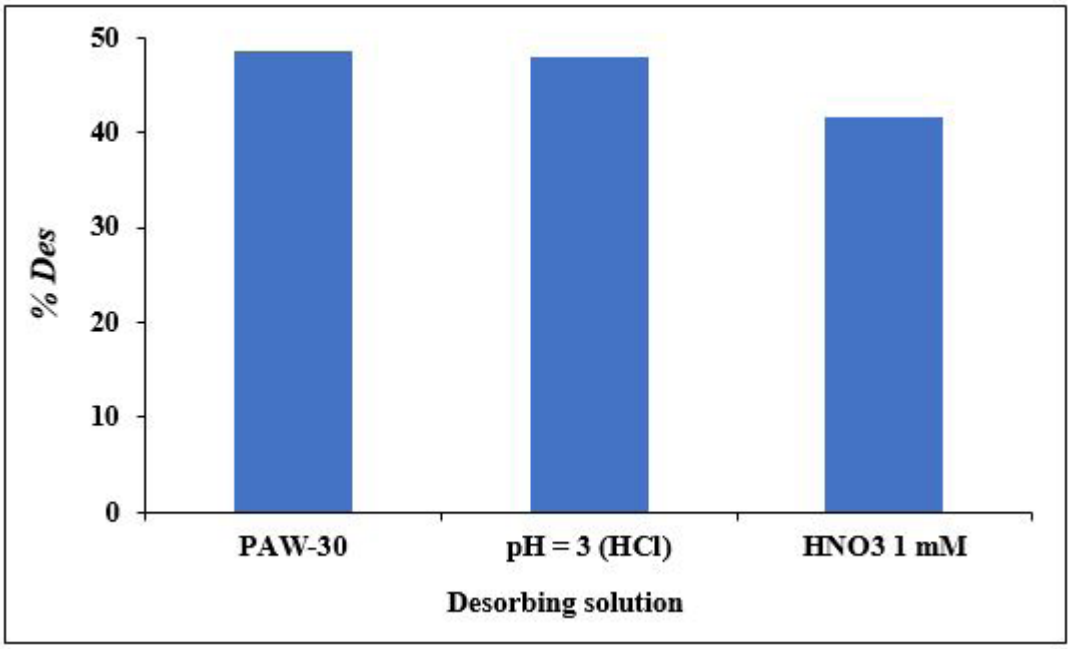

Figure :8 Removal percentage for desorption of MB dye from MS in different desorbing solutions

As for the remaining fraction of pre-adsorbed MB, it could still be linked to the sawdust by a different mechanism of cation exchange, such as chemisorption or a chemical interaction. Indeed, Chen at al. [46] showed that adsorption process might be chemisorption if the dye adsorbed can be desorbed by weak acid, however PAW can be considered as a weak acid. To better assess the observed non-desorbed MB, a three-step desorption was performed on the same material previously loaded by MB. After each stage, the desorbing solution was discarded, and MS was introduced in a freshly PAW solution. After the 4.65 mg/g desorbed in the first trial, 1.46 mg/g was desorbed in the second, and 0.42 mg/g was obtained in the third. At the end of the third step, the solution resulting from desorption was practically colorless, proof that the desorbed MB was there in very small quantity. The total percentage of the desorbed MB does not exceed 68% of the amount of the MB initially present on MS. All these results highlight that a part of the MS adsorption could be rather chemical and irreversible.

MB decolorization by PAW

Given the unsuccessful attempts for the total desorption of MB from MS, the oxidizing effect of PAW may have intervened in the degradation of the dye during desorption process. Indeed, previous studies have shown that plasma itself could be used to regenerate the adsorbent while degrading the pollutant [45, 47]. We carried out a simple test by putting MB dye into contact with PAW and the degradation of the MB was followed by measuring its absorbance for different contact times. For this, 2 mL of 250 $mg.L^{-1}$ dye was mixed with 48 mL of PAW so that the initial concentration was 10 $mg.L^{-1}$. The results of this trial are presented in Fig. 9.

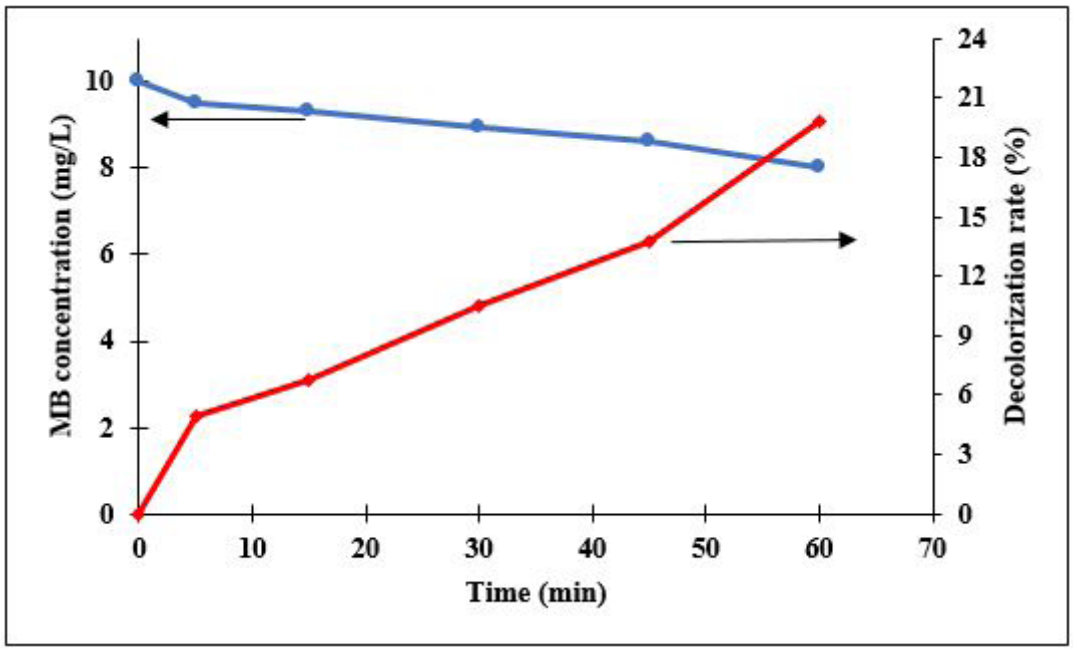

Figure :9 Evolution of initial MB concentration and decolorization rate as a function of PAW treatment time

There was decolorization, although slight, of the initial MB, but which changes over time, with a rate of around 20% for 1 h of treatment. The same experiment, using HCl solution (at pH 3) instead of PAW solution, did not show any MB decolorization after 1h of contact (data not shown). This result would indicate that MB was also degraded by PAW during desorption. This result agrees with previous studies demonstrating that MB could be degraded during the plasma treatment under direct discharge [48], although in addition to the active species present in PAW, the degradation under active plasma discharge also induces the effect of other parameters such as UV, the presence of highly reactive radicals, etc.

Kinetic study of desorption

The experimental data obtained for the desorption study were used to determine if the process followed a suitable kinetic model. The pseudo-first-order and pseudo-second-order kinetic equations can be adapted for desorption by assuming that the rate of desorption is proportional to the number of MB molecules-filled sites and the square of the number of MB molecules-filled sites, respectively. The pseudo-first-order and pseudo-second-order kinetic linearized equations are given by Eq. (20) and Eq. (21) respectively:

$$\ln(q_{e,des} - q_{Dt}) = -k_{1D}.t + \ln(q_{e,des}) \quad (20)$$

$$\frac{t}{q_{Dt}} = \frac{t}{q_{e,des}} + \frac{1}{k_{2D}.q_{e,des}^2} \quad (21)$$

where, q_{Dt} (mg/g) and $q_{e,des}$ (mg/g) are the amount of MB dye molecules that have been desorbed and the amount of desorbed MB dye molecules at desorption equilibrium, respectively. k_{1D} (min^{-1}) and k_{2D} (g/mg.min) are the reaction rate constants for the pseudo-first-order and pseudo-second-order desorption reaction, respectively.

Plotting ln ($q_{e,des} - q_{Dt}$) *vs.* t and t/q_{Dt} *vs* t gave the different constants recorded in Table 4.

The conformity between the experimental data and the model-predicted values were determined from coefficients of determination. Higher model R^2-values (i.e. 0.9999 for all temperatures tested) demonstrate that the pseudo-second-order model is significant. The pseudo-second-order equation showed more accurate prediction of equilibrium desorption capacities ($q_{e,desII}$ calculations close to experimental values) than the pseudo-first order equation. Thus, based on the kinetic results, desorption was found to follow pseudo-second-order reaction. Daneshvar et al. [43] also showed that desorption of MB from macroalga using HCl followed

a pseudo-second-order kinetic model. The pseudo-second-order is based on the assumption that desorption process (in this case) is the rate-limiting-step, involving valence forces through the sharing or exchanging of electrons adsorbent and adsorbate [49]. It resulted that adsorption and desorption process followed the same kinetic model, but with higher rate constants for the adsorption process.

T (K)	$q_{e,des,\,exp}$ (mg.g^{-1})	Pseudo-first-order			Pseudo-second-order		
		K_{1D} (min^{-1})	R^2	$q_{e,\,desI}$ (mg.g^{-1})	K_{2D} (g/(mg.min))	R^2	$q_{e,\,desII}$ (mg.g^{-1})
298	4.31	0.0337	0.6751	1.68	0.16	0.9999	4.42
313	4.37	0.0331	0.5976	1.45	0.21	0.9998	4.43
323	4.47	0.0395	0.6491	1.33	0.22	0.9999	4.52
333	4.49	0.0419	0.6779	1.34	0.21	0.9999	4.55

Table :4 Pseudo-first-order and pseudo-second-order parameters at various initial temperatures for desorption of MB dye from MS

Reusability tests

The substantial and fast desorption process indicates that the MS could be facilely regenerated for repeated dye removal applications. Thus, MS can be used in the multiple adsorption/desorption cycles by applying desorption process. Three adsorption/desorption cycles were carried out using the same sample of MS in ambient conditions. Fig. 10 shows the rate of adsorption and desorption of each cycle.

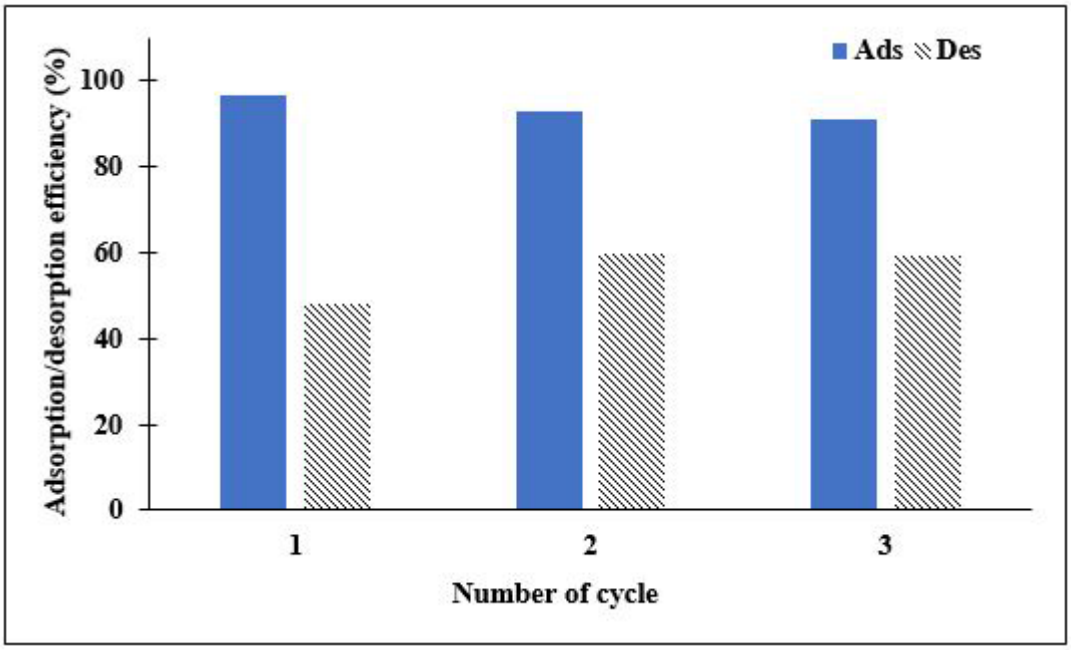

Figure 10: Adsorption efficiency (%) of MS towards MB removal up to three successive regeneration cycles by PAW treatment

From the first to second, the adsorption efficiency slightly decreased from 95.54% to 92.92%, while between the two experiments, 47.93% of adsorbed MB was desorbed. The capacity of adsorption remains at high level, even if all MB was probably not desorbed. The same trend was observed from the second to the third cycle. We also noted that the desorption efficiency increased with the number of cycle: from 47.93% (first cycle) to 59.71% (third cycle). As between two consecutive cycles, MB was not totally desorbed, this demonstrates that, the higher quantity of MB loaded into MS is, the higher percentage of MB desorption is. Globally, the regeneration investigation of MB adsorption using PAW solution showed that negligible decrease in the removal efficiency was observed up to three cycles. PAW solution could thus be considered as a non-aggressive solution as demonstrated in previous research concerning the decontamination of surfaces [37]. Literature reported some successful regenerated studies for low-cost adsorbents, using chemical as desorbing agent, but sometimes associated to a modification of the original sorbent [43]. Exposing the contaminated adsorbents to plasma also showed interesting results in regeneration [45, 47, 50] with adsorption efficiency

higher than 80% even after five cycles. However, the plasma itself, contrary to PAW, has the disadvantage that it can damage/modify deeply the surface of adsorbents [21] and then modifies the initial structural properties of the material. Indeed, the excited species generated by non-thermal plasma may interact with solid surfaces placed in the plasma and lead to a variety of possible reactions, such as etching, cross-linking and chemical modification.

Conclusions

The present study has established the efficiency of MS as suitable low-cost adsorbent for effective removal of MB dye from aqueous solutions. The equilibrium time was found to be independent of adsorbent dose. The adsorption process follows pseudo-second-order kinetic model with high value of R^2 (0.999). Although MS are abundant adsorbent for pollutant removal, the disposal of pollutant-loaded-adsorbent is another challenge in wastewater treatment studies. Given that, the present study also reports the results of MB dye desorption using a new method namely Plasma activated water (PAW). This activated solution was obtained by exposing distilled water to humid air plasma. The key role of the pH of PAW during desorption was demonstrated through comparison with HCl and HNO_3 capacity desorption. The result indicates that H^+ ion exchange takes place in the acidic medium with adsorbed MB dye molecules on the surface of MS. PAW also showed ability to slowly decolorize MB during the desorption process. Desorption kinetic data were fitted well to pseudo-second-order model with high value of R^2 (0.9999). The reusability of MS during three consecutive adsorption/desorption cycles was successfully achieved. The findings of this study suggest that one hand, MS can be a serious candidate for the adsorption of basic dye from aqueous solution and the other hand that PAW can be used as an efficient desorbing agent for MS regeneration, thus eliminates and minimizes the quantity of using chemical substances. Moreover, PAW offers a better versatile solution and a possibility to treat material far from the place of its manufacturing.

Acknowledgment

Thanks to the International Foundation of Sciences (IFS) for the provision of equipment through the scholarship (N°: W/4219 -1) to Dr. Nzali serge. Special thanks to "*Laboratoire d'Electrochimie Interfaciale et de Chimie Analytique*" of University of Rouen (France) for the collaboration.

This research did not receive any specific grant from funding agencies in the public, commercial, or not-for-profit sectors.

References

1.Rafatullah M, Sulaiman O, Hashim R, Ahmad A (2010) Adsorption of methylene blue on low-cost adsorbents : A review. J Hazard Mater 177 : 70-80.

2. Ghezzar MR, Abdelmalek F, Belhadj M, Benderdouche N, Addou A, et al. (2009) Enhancement of the bleaching and degradation of textile wastewaters by Gliding arc discharge plasma in the presence of TiO2 catalyst. J Hazard Mater 164 : 1266-74.

3. Njiki A, Kamgang-Youbi G, Laminsi S, Lontsi CD, Payom G, Nola M, Ngameni E, et al. (2016) Gliding arc discharge-assisted biodegradation of crystal violet in solution with Aeromonas hydrophila strain. Int J Environ Sci Technol 13 : 263-74.

4. Gupta VK, Ali I, Saleh TA, Nayak A, Agarwal S, et al. (2012) Chemical treatment technologies for waste-water recycling- an overview. RSC Adv 2 : 6380-8.

5. Tsang DCW, Hu J, Liu MY, Zhang WH, Lai KCK, Lo IMC (2007) Activated carbon produced from waste wood pallets: Adsorption of three classes of dyes. Water Air Soil Pollut 184 : 141–55.

6. Yan C, Wang C, Yao J, Zhang L, Liu X (2009) Adsorption of methylene blue on mesoporous carbons prepared using acid-and alkaline-treated zeolite X as the template. Colloids Surf A 333 : 115–9.

7. Hor KY, Chee JMC, Chong MN, Jin B, Saint C, Poh PE, Aryal R (2016) Evaluation of physicochemical methods in enhancing the adsorption performance of natural zeolite as low-cost adsorbent of methylene blue dye from wastewater. J Clean Prod 118 : 197–209.

8. Boyom TFW, Nzali S, Kamgang Youbi G, Tiya Djowe A, Kuete Saa D, Acayanka E, Laminsi S, Gaigneaux EM (2017) Gliding arc plasma synthesis of MnO2 nanorods for the plasma-catalytic bleaching of azoïc Amaranth red dye. Top Catal 60 : 962–72.

9. Sop Tamo B, Kamgang-Youbi G, Acayanka, Simo LM, Tiya-Djowe A, Kuete-Saa D, Laminsi S, Tchadje L (2016) Plasma chemical functionalisation of a cameroonian kaolinite clay for a greater hydrophilicity. Plasma Chem Plasma Process 36 : 1449–69.

10. Karim AB, Mounir B, Hachkar M, Bakasse M, Yaacoubi A (2017) Adsorption/desorption behavior of cationic dyes on Moroccan clay: equilibrium and mechanism. J Mater Environ Sci 8 : 1082-96.

11. Takam B, Acayanka E, Kamgang-Youbi G, Pedekwang MT, Laminsi S (2017) Enhancement of sorption capacity of cocoa shell biomass modified with non-thermal plasma for removal of both cationic and anionic dye from aqueous solution. Environ Sci Pollut Res 24 : 16958-70.

12. Gupta VK, Suhas (2009) Application of low-cost adsorbents for dye removal – a review. J Environ Manag 90 : 2313–42.

13. Gouamid M, Ouahrania MR, Bensacib MB (2013) Adsorption equilibrium, kinetics and thermodynamics of methylene blue from aqueous solutions using Date Palm Leaves. Energy Procedia 36 : 898–907.

14. Jeyagowri B, Yamuna RT (2015) Biosorption of methylene blue from aqueous solutions by modified mesoporous simarouba glauca seed shell powder. Global NEST J 17 : 701–15.

15. Kushwaha AK, Gupta N, Chattopadhyaya MC (2014) Removal of cationic methylene blue and malachite green dyes from aqueous solution by waste materials of Daucus carota. J Saudi Chem Soc 18 : 200–7.

16. Shakoor S, Nasar A(2016) Removal of methylene blue dye from artificially contaminated water using citrus limetta peel waste as a very low-cost adsorbent. J Taiwan Inst Chem Eng 66 : 154–63.

17. Lim LBL, Priyantha N, Tennakoon DTB, Chieng HI, Dahri MK, Suklueng M (2017) Breadnut peel as a highly effective low-cost biosorbent for methylene blue : Equilibrium, thermodynamic and kinetic studies. Arabian J Chem 10 : 3216–28.

18. Kallel F, Chaari F, Bouaziz F, Bettaieb F, Ghorbel R, Chaabouni SE (2016) Sorption and desorption characteristics for the removal of a toxic dye, methylene blue from aqueous solution by a low cost agricultural by-product. J Mol Liq 219 : 279–88.

19. M'hamdi AI, Kandri NI, Zerouale A (2017) Adsorption study of the methylene blue on sawdust beech and red wood. J Mater Environ Sci 8 : 2816–31.

20. Djilali Y, Elandaloussi EH, Aziz A, Ménorval LC (2016) Alkaline treatment of timber sawdust: A straightforward route toward effective low-cost adsorbent for the enhanced removal of basic dyes from aqueous solutions. J Saudi Chem Soc 20 : 241–9.

21. Akrout H, Jellali S, Bousselmi L (2015) Enhancement of methylene blue removal by anodic oxidation using BDD electrode combined with adsorption onto sawdust. Comptes Rendus Chimie 18 : 110–20.

22. Wang Y, Zhu L, Jiang H, Hu F, Shen X (2016) Application of longan shell as non–conventional low-cost adsorbent for the removal of cationic dye from aqueous solution. Spectrochim. Acta A 159 : 254–61.

23. Salazar-Rabago JJ, Leyva-Ramos R, Rivera-Utrilla J, Ocampo-Perez R, Cerino-Cordova FJ (2017) Biosorption mechanism of methylene blue from aqueous solution onto white pine (Pinus durangensis) sawdust: Effect of operating conditions. Sustain Environ Res 27 : 32–40.

24. Ofomaja AE (2008) Kinetic study and sorption mechanism of methylene blue and methyl violet onto Mansonia (Mansonia altissima) wood sawdust. Chem Eng J 143 : 85–95.

25. Rangabhashiyam S, Lata S, Balasubramanian P (2018) Biosorption characteristics of methylene blue and malachite green from simulated wastewater onto Carica papaya wood biosorbent. Surf Interfaces 10: 197–215.

26. Bhattacharyya KG, Sharma A (2005) Kinetics and thermodynamics of methylene blue adsorption on Neem (Azadirachta indica) leaf powder. Dyes Pigm 65 : 51–9.

27. Meng W, Ma Z, Shu J, Li B, Su P, Wang R, Chen M, Liu Z, Ai K (2022) Efficient adsorption of methylene blue from aqueous solution by hydrothermal chemical modification phosphorus ore flotation tailings. Sep Purif Technol 281 : 119496.

28. Sukhatskiy Y, Sozanskyi M, Shepida M, Znak Z, Parag, Gogate R (2022) Decolorization of an aqueous solution of methylene blue using a combination of ultrasound and peroxate process. Sep Purif Technol 288 : 120651.

29. Nko'o AMC, Avom J, Mpon R, Ketcha-Mbadcam J, Belibi-Belibi PD (2013) Valorization of a cameroonian species: Moabi (Baillonella Toxisperma) into activated carbons. Int J Cur Res Rev 5 : 1–10.

30. Brisset JL, Moussa D, Doubla A, Hnatiuc E, Hnatiuc B, Kamgang-Youbi G, Herry JM, Naïtali M, Bellon-Fontaine MN (2008) Chemical reactivity of discharges and temporal post-discharges in plasma treatment of aqueous media. Example of gliding discharge treated solutions. A review. Ind Eng Chem Res 47 : 5761–81.

31. Abdelmalek F, Torres RA, Combet E, Petrier C, Pulgarin C, Addou A (2008) Gliding Arc Discharge (GAD) assisted catalytic degradation of bisphenol A in solution with ferrous ions. Sep Purif Technol 63 : 30–7.

32. Burlica R, Kirkpatrick MJ, Locke BR (2006) Formation of reactive species in gliding arc discharges in water. J Electrost 64 : 35–43.

33. Kamgang-Youbi G, Herry JM, Bellon-Fontaine MN, Brisset JL, Doubla A, Naïtali M (2007) Evidence of the temporal post-discharge decontamination of bacteria by gliding electric discharges: application to Hafnia alvei. Appl Environ Microbiol 73 : 4791–6.

34. Kamgang–Youbi G, Herry JM, Brisset JL, Bellon-Fontaine MN, Doubla A, Naïtali M (2008) Impact on disinfection efficiency of cell load and of "planktonic/adherent/detached state : case of Hafnia alvei inactivation by plasma activated water. Appl Microbiol Biotechnol 81 : 449–57.

35. Kamgang–Youbi G, Herry JM, Meylheuc T, Brisset JL, Bellon-Fontaine MN, Doubla A, Naïtali M (2009) Microbial inactivation using plasma-activated water obtained by gliding electric discharges. Lett Appl Microbiol 44 : 13–8.

36. Naïtali M, Kamgang-Youbi G, Herry JM, Bellon-Fontaine MN, Brisset JL (2010) Combined effect of long-living chemical species during microbial inactivation using atmospheric plasma-treated water. Appl Environ Microbiol 76 : 7662–4.

37. Kamgang-Youbi G, Herry JM, Meylheuc T, Laminsi S, Naïtali M (2018) Microbial decontamination of stainless steel and polyethylene surfaces using GlidArc plasma activated water without chemical additives. J Chem Technol Biotechnol 93 : 2544–51.

38. Ofomaja AE, Ho Y (2008) Effect of temperature and pH on methyl violet biosorption by Mansonia wood sawdust. Bioresour Technol 99 : 5411–7.

39. Acayanka E, Tarkwa JB, Laminsi S (2018) Evaluation of energy balance in a batch and circulating non-thermal plasma reactors during organic pollutant oxidation in aqueous solution. Plasma Chem Plasma Process 39 : 75–87.

40. Nanseu-Njiki CP, Dedzo GK, Ngameni E (2010) Study of the removal of paraquat from aqueous solution by biosorption onto Ayous (Triplochiton schleroxylon) sawdust. J Hazard Mater 179 : 63–71.

41. Ho YS, McKay G (1999) Pseudo-second order model for sorption processes. Process Biochem 34 : 451–65.

42. Wu FC, Tseng RL, RS Juang (2009) Characteristics of Elovich equation used for the analysis of adsorption kinetics in dye–chitosan systems. Chem Eng J 150 : 366–73.

43. Daneshvar E, Vazirzadeh A, Niazi A, Kousha M, Naushad M, Bhatnagar A (2017) Desorption of Methylene blue dye from brown macroalga : Effects of operating parameters, isotherm study and kinetic modeling. J Clean Prod 152 : 443–53.

44. Zheng L, Su Y, Wang L, Jiang Z (2009) Adsorption and recovery of methylene blue from aqueous solution through ultrafiltration technique. Sep Purif Technol 68 : 244–9.

45. Zhou R, Zhou R, Zhang X, Tu S, Yin Y, Yang S, Ye L (2016) An efficient bio-adsorbent for the removal of dye : Adsorption studies and cold atmospheric plasma regeneration. J Taiwan Inst Chem Eng 68 : 372–8.

46. Chen YG, Ye WM, Yang XM, Deng FY, He Y (2011) Effect of contact time, pH, and ionic strength on Cd(II) adsorption from aqueous solution onto bentonite from Gaomiaozi, China. Environ Earth Sci 64 : 329–36.

47. Iervolino G, Sacco O, Vaiano V, Palma V (2019) Non-thermal plasma technology for the effective regeneration of macroscopic adsorbent materials used in the removal of Patent Blue V dye from aqueous solutions. Chem Eng Trans 73 : 151–6.

48. Yamada M, Wahyudiono, Machmudah S, Kanda H, Goto M (2020) Nonthermal atmospheric pressure plasma for methylene blue dye decolorization by using slug flow reactor system. Plasma Chem Plasma Process 40 : 985–1000.

49. Njikam E, Schiewer S (2012) Optimization and kinetic modeling of cadmium desorption from citrus peels : a process for biosorbent regeneration. J Hazard Mater 213–214 : 242–8.

50. Qu GZ, Li J, Wu Y, Li GF, Li D (2009) Regeneration of acid orange 7-exhausted granular activated carbon with dielectric barrier discharge plasma. Chem Eng J 146 : 168–73.